Oncogene (2002) 21, 5097–5107

www.nature.com/onc

Mammary tumors in mice conditionally mutant for *Brca1* exhibit gross genomic instability and centrosome amplification yet display a recurring distribution of genomic imbalances that is similar to human breast cancer

Zoë Weaver[1,5], Cristina Montagna[1], Xiaoling Xu[2], Tamara Howard[3], Massimo Gadina[4], Steven G Brodie[2], Chu-Xia Deng[2] and Thomas Ried*[,1]

[1]*Genetics Branch, Center for Cancer Research, National Cancer Institute/NIH, Bethesda, Maryland, USA;* [2]*Genetics of Development and Disease Branch, National Institute of Diabetes, Digestive and Kidney Diseases/NIH, Bethesda, Maryland, USA;* [3]*Cold Spring Harbor Laboratory, Cold Spring Harbor, New York, USA;* [4]*National Institute of Arthritis and Musculoskeletal and Skin Diseases/NIH, Bethesda, Maryland, USA*

***BRCA1* mutation carriers have an increased susceptibility to breast and ovarian cancer. Excision of exon 11 of *Brca1* in the mouse, using a conditional knockout (Cre-loxP) approach, results in mammary tumor formation after long latency. To characterize the genomic instability observed in these tumors, to establish a comparative map of chromosomal imbalances and to contribute to the validation of this mouse model of breast cancer, we have characterized chromosomal imbalances and aberrations using comparative genomic hybridization (CGH), and spectral karyotyping (SKY). We found that all tumors exhibit chromosome instability as evidenced by structural chromosomal aberrations and aneuploidy, yet they display a pattern of chromosomal gain and loss that is similar to the pattern in human breast carcinomas. Of note, nine of 15 tumors exhibited a gain of distal chromosome 11, a region that is orthologous to human chromosome 17q11-qter, the mapping position of *Erbb2*. However, our analysis suggests that genes distal to *Erbb2* are the main targets of amplification. Four of the tumors also exhibited a copy number loss of proximal chromosome 11 (11A-B), a region orthologous to human 17p. In eight of the tumors we observed whole or partial gain of chromosome 15 centering on 15D2-D3 (orthologous to human chromosome 8q24), the map location of the c-*Myc* gene, and six of the tumors exhibited copy number loss of whole or partial chromosome 14, including 14D3, the map location of *Rb1*. We conclude that despite the tremendous shuffling of chromosomes during the course of mammalian evolution, the pattern of genomic imbalances is conserved between *BRCA1*-associated mammary gland tumors in mice and humans. Western blot analysis showed that while p53 is absent or mutated in some tumors, at least two tumors revealed wild-type protein, suggesting that other genetic events may lead to tumorigenesis. Similar to *BRCA1*-deficient mouse embryonic fibroblasts, the tumor cells contained supernumerary functional centrosomes with intact centrioles whose presence results in multipolar mitoses and aneuploidy.**

Oncogene (2002) **21,** 5097–5107. doi:10.1038/sj.onc.1205636

Keywords: Brca1; mouse models; SKY; genomic imbalances; centrosome

Introduction

Loss of one copy of the *BRCA1* tumor suppressor gene is responsible for increased susceptibility to familial breast and ovarian cancer. Functional analyses of BRCA1 revealed its involvement in DNA damage-induced repair and regulation of transcription (Deng and Scott, 2000). BRCA1 co-localizes with the RAD50/MRE 11/NBS1 repair complex in nuclear foci (Zhong *et al*., 1999), and associates with the SWI/SNF chromatin-remodeling complex (Bochar *et al*., 2000). This is consistent with the hypothesis that the genomic instability observed in Brca1-null cells is due to defects in homologous recombination. Thus, failure to repair double-strand breaks results in an accumulation of genetic damage in Brca1-null cells. If this damage affects gatekeeper genes downstream of *BRCA1*, mutant cells can bypass cell-cycle checkpoints and apoptosis, which results in continued proliferation and the development of breast cancer (Khanna and Jackson, 2001).

Several studies have made progress towards defining the nature of additional mutations that are required for malignant transformation of *BRCA1*-deficient cells. For instance, comparative genomic hybridization (CGH) of breast tumors from BRCA1 mutation carriers revealed a distinct pattern of genomic imbalances, providing evidence that genomic imbalances differ from those observed in sporadic breast cancers (Tirkkonen *et al*., 1997). Detailed karyotype analysis of a breast cancer cell line homozygous for a *BRCA1* mutation revealed multiple chromosomal aberrations,

*Correspondence: T Ried, Genetics Branch, Center for Cancer Research, National Cancer Institute/NIH, 50 South Drive, Room 1306, Bethesda, Maryland, MD 20892-8010, USA;
E-mail: riedt@mail.nih.gov
[5]Current address: Avalon Pharmaceuticals, 19 Firstfield Road, Gaithersburg, Maryland, MD 20878, USA
Received 14 February 2002; revised 24 April 2002; accepted 29 April 2002

including a high degree of aneuploidy, loss of wild-type *p53*, acquired homozygous deletion of the *PTEN* tumor suppressor gene, and loss of heterozygosity at multiple loci known to be involved in the pathogenesis of breast cancer (Tomlinson *et al*., 1998).

Mouse models of human cancers are enormously important tools to dissect genetic pathways of tumorigenesis. Several groups have therefore attempted to recapitulate mammary gland tumorigenesis in mice deficient for *Brca1* (Deng and Brodie, 2001). However, homozygous loss of *Brca1* results in embryonic lethality at day E5.5–18.5 (Gowen *et al*., 1996; Hakem *et al*., 1996; Liu *et al*., 1996; Ludwig *et al*., 1997; Shen *et al*., 1998). Mouse embryonic fibroblast cells (MEFs), which carry a targeted deletion in exon 11 of *Brca1*, exhibit chromosome instability, amplification of functional centrosomes, and are defective in the G_2-M checkpoint (Xu *et al*., 1999b). However, the conditional elimination of *Brca1* in the mammary gland epithelium using a Cre-loxP approach results in blunted ductal morphogenesis and tumor formation after approximately 1 year (Xu *et al*., 1999a). The long latency suggests that additional genetic changes are necessary for tumorigenesis. For instance, loss of p53 accelerated the formation of mammary tumors (Xu *et al*., 1999a). To characterize the genomic instability observed in these tumors, to establish a comparative map of chromosomal imbalances and to contribute to the validation of this mouse model of breast cancer, we have mapped DNA gains and losses and characterized chromosomal aberrations using comparative genomic hybridization (CGH) and spectral karyotyping (SKY). As a potential cause for chromosomal aneuploidy, the integrity of centrosomes was assessed by immunocytochemistry and electron microscopy. Additionally, as breast cancers in *BRCA1* carriers typically contain either a *p53* mutation and/or p53 protein accumulation (Schuyer and Berns, 1999) we analysed several of the tumors for presence of the p53 gene and protein. The results reveal striking similarities between this mouse model and human breast carcinomas precipitated by mutations in the *BRCA1* tumor suppressor gene.

Results

CGH of primary Brca1-deficient tumors reveals a pattern of chromosomal gains and losses similar to human breast cancer

To analyse chromosomal copy number changes in Brca1-deficient tumors, we performed CGH using genomic DNA from 11 *Brca1* conditional mutant mammary gland tumors ($Brca1^{Ko/Co}$ *Wap-Cre* or *MMTV-Cre*), designated brt-1 through brt-11, and from four *Brca1* conditional tumors in a p53 mutant background ($Brca1^{Ko/Co}$*Wap-Cre*$Trp53^{+/-}$), designated pbrt-1 through pbrt-4. A summary of chromosomal copy number changes is presented in Figure 1. Each chromosome was involved in at least one gain or loss, but the distribution of genomic imbalances was non-random, which allows for a comparison with chromosomal copy number changes in human breast cancer. The number of chromosome copy alterations ranged from two to 21 per tumor, and the average number of copy alterations (ANCA, Ried *et al*., 1999) amounts to 8.1 per tumor. We did not observe significantly different ANCA values for the *Brca1* tumors in a $p53^{+/-}$ background (ANCA = 7.25) compared to the *Brca1* mutant alone, suggesting that there was no increase in chromosomal instability. The most consistent changes in both groups were gain of distal chromosome 11, partial gain of chromosome 15, loss of distal chromosome 14 and chromosome 4, and gain of the X-chromosome.

Nine of 15 tumors (brt-2, -4, -5, -6, -9, -10, -11, and pbrt-1 and -4) exhibited a gain of distal chromosome 11 (Figure 1). The common portion gained centered on 11D-E, a region that is orthologous to human chromosome 17q11-qter. Four of the tumors (brt-5, -9, -10 and pbrt-1) also exhibited a copy number loss of proximal chromosome 11 (11A-B), a region orthologous to human 17p that may include the p53 gene (which maps to 11B2-C).

In eight of the tumors (brt-1, -2, -5, -6, -8, -10, pbrt-1, -2) we observed whole or partial gain of chromosome 15 centering on 15D2-D3 (orthologous to human chromosome 8q24), the map location of the c-*Myc* gene. Even in a tumor in which the entire chromosome 15 was gained (pbrt-2), band 15D2-D3 was relatively amplified (Figure 1).

Six of the tumors (brt-4, -5, -6, -7, -9, -10) exhibited copy number loss of whole or partial chromosome 14, including 14D3, the map location of *Rb1*. Other copy number changes included loss of whole or distal chromosome 4, gain of the X-chromosome, and loss of whole or partial chromosome 12.

As the CGH results indicated an accumulation of genetic defects in the tumor cells, we wished to determine if the observed aberrations would remain stable in cells at late passage. Tumor brt-5 was expanded to passage 31 and CGH was applied to compare to results from the primary tumor material. The cultured cells contained nine additional gains and four additional losses of chromosomal material (data not shown). Moreover, the amplifications that were mapped to chromosome 11D-E and chromosome 15D exhibited higher-level copy number increases relative to the primary tumor. Despite this chromosomal instability in dividing cells, the majority of the aberrations found in the primary tumor is continuously selected for and therefore maintained even during ongoing cell culture. Clearly the selective pressures are different for cells growing in culture than for cells dividing in the context of mammary tissue. However, we can surmise that the consistent aberrations seen at the genomic level are the ones that give the cells a growth advantage, and additional genetic changes necessary for growth in tissue culture may not be visible at the genomic level. This is consistent with results obtained from human epithelial cancer cell lines (Ghadimi *et al*., 1999).

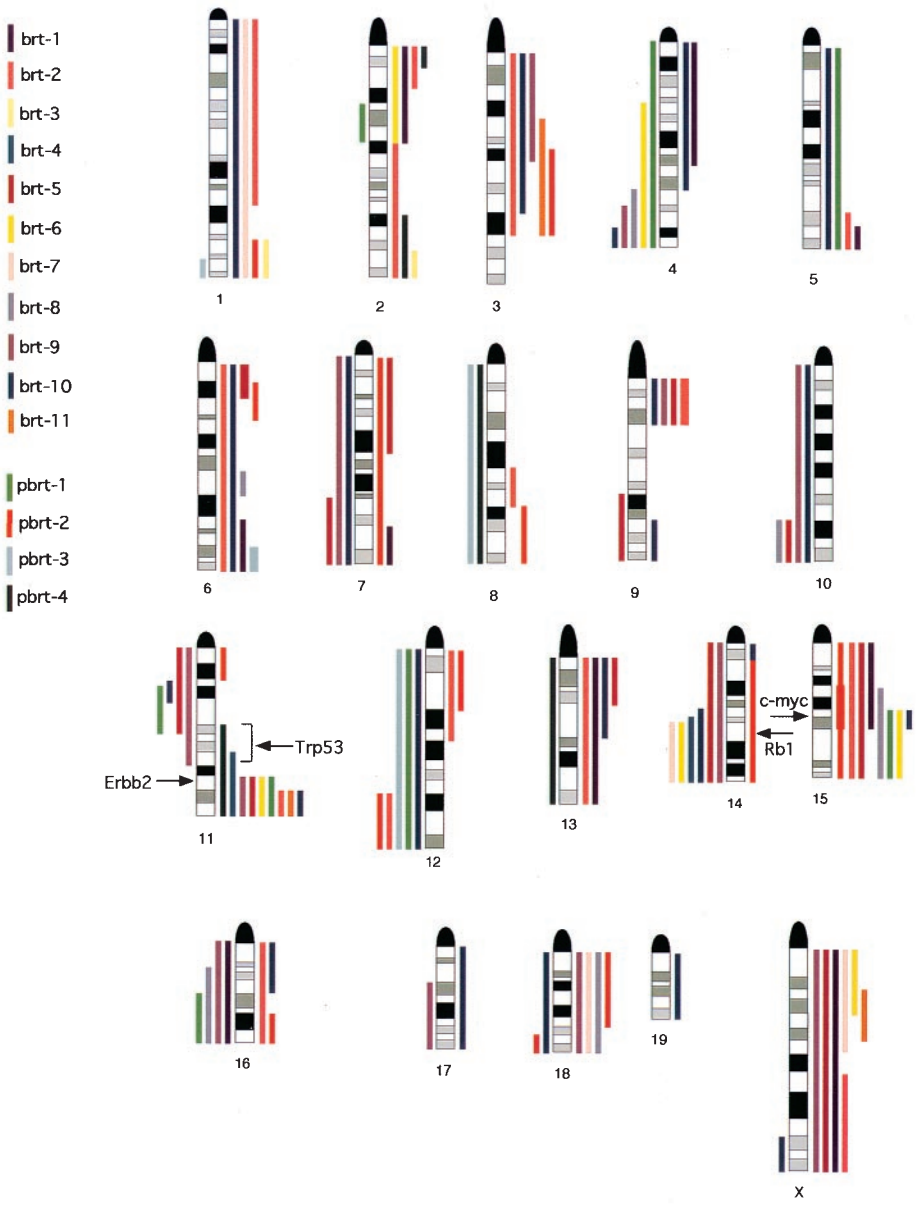

Figure 1 Summary of CGH analysis of 15 *Brca1* conditional mutant mammary tumors. Bars on the right side of the chromosome ideograms indicate gain and bars on the left side loss of genetic material. All gains and losses for a single tumor are represented in the same color. Bold lines denote high-level copy number increases. The chromosomal map position of the tumor suppressor genes *Trp53* and *Rb1* and the oncogenes *Erbb2* and c-*myc* is indicated

SKY analysis of Brca1-deficient tumors shows gross chromosomal instability yet recurrent aberrations

In order to examine the chromosomal mechanisms that result in the recurring copy number changes found in the $Brca1^{Ko/Co}$ mammary tumors, we applied SKY to tumor metaphase chromosomes. Although we were unable to obtain metaphases from primary cultures of every tumor, we obtained karyotype data from passage 0 or 1 from tumors brt-1, -2, -5, -9 and -10, and $Brca1^{Ko/Co}Trp53^{+/-}$ tumor pbrt-1 and pbrt-3 (Table 1). In only one case (brt-5) was SKY not performed until a later passage (p31).

Every tumor displayed structural aberrations and numerical chromosomal aberrations, but different degrees of multiclonality. Only two of the tumors (brt-1 and -2) were largely clonal in origin; all others had individual 'marker' chromosomes that were present in many or most of the cells accompanied by numerous additional sporadic aberrations in individual cells, indicative of a high degree of chromosomal instability. Chromosome and chromatid breaks were observed in many cases, and in some instances chromosomes appeared to be captured in the process of rearranging (Figure 2).

Tumor brt-2 serves as a representative example of SKY analysis of a primary culture. The karyotype included structural aberrations such as insertions, deletions, dicentric chromosomes, and chromatid breakage (Figure 2). Despite this considerable degree

Table 1 *SKY* and *FISH* results for *Brca1$^{Ko/Co}$Wap-Cre and Brca1$^{Ko/Co}$Wap-CreTrp53$^{+/-}$ tumors*

Tumor #	*Ploidy*[b]	*SKY (recurrent aberrations)*[c]	*Chromosome 11 paint*[d]	*Trp53 FISH*[e]	*Erbb2 FISH*[f]
brt-1(p0)[a]	2n	t(7F; 11B); T(11B; 7F)	confirms T(7;11), T(11;7)	*Trp53* appears to be at T(7;11) breakpoint	nd
brt-1(p31)	<3n-4n>	T(7;11)	3–4 copies del(11)		*Erbb2* telomeric to the breakpoint on chr11
brt-2	3n	Del(1), T(3;12), T(6;9;8), T(8;19),	1–3 normal 11, Del(11),	*Trp53* on normal 11,	*Erbb2* on normal 11,
	clonal	Dic(ls(8;9)), T(9;6), Del(11), T(11;13), T(13;11), Del(X)	1–3 copies of a translocation of ~1 band of 11 to either cent or tel or partner chrom (too small to see by SKY)	not on translocated pieces	not on translocated pieces
brt-3	6n	nd	3 T(11D-E:?), 3 Del(11), 4-7 T(?;11)	nd	no *Erbb2* on T(11;?), Del(11) piece has *Erbb2*, piece of 11 in T(?;11) has *Erbb2*
brt-5(p0)	3n	nd	nd	nd	nd
brt-5(p31)	3n	T(6;13), T(7;13), T(8;19), T(9;18), Del(11), T(13;16) T(13;7), T(14;12), T(14;19), T(16;2)	3 normal chr 11; 1–3 copies of a Del(11)	*Trp53* on normal 11 not on Del(11)	*Erbb2* on normal 11 *Erbb2* signal on Del(11) i.e., Del(11) = Del(11B-C)
brt-6	*clone a*: 3n *clone b*: 4n		*clone a*: 2 normal 11, 2 Del(11) *clone b*: 4 normal 11,	nd	*Erbb2* on normal 11 Del(11) has *Erbb2*
brt-9	<3n> 57-67 chr	T(1;2) x2, T(2;1) x2, Del(3) x2, R(4;X), D_I(9) x2, Del(11) x2	*clone a*: 2 normal 11, 2 Del(11) *clone b*: 1 normal 11, 2 Del(11),	nd	*clone a*: *Erbb2* on normal 11 *Erbb2* on Del(11), i.e. interstitial del *clone b*: *Erbb2* on normal 11 *Erbb2* on Del(11) *Erbb2* on T(?;11) no *Erbb2* on T(11;?)
brt-10	*clone a*: 6n *clone b*: 3n	Del(4), T(6;11), T(11;6?), Del(11) × 3	*clone a*: 4 normal 11, 2 Del(11), 4 T(?;11) *clone b*: 1 normal 11, 2 Del(11), 2 T(?,11), 1 ls(11;?)	*Trp53* on normal 11 in both *clone a* and *clone b* not on deleted or translocated pieces	*clone a*: *Erbb2* on 1 normal 11 3 'normal' 11 have no *Erbb2* signal, no *Erbb2* on 2 Del(11), *Erbb2* signal on 4 T(?;11), *clone b*: *Erbb2* signal on 2 T(?;11), *Erbb2* signal on ls(11;?) no *Erbb2* on 'normal' 11 no *Erbb2* on Del(11)
pbrt-1	<3n-6n> 68-127 chr	Del(4), T(6;11), Del(11)	nd	nd	nd
pbrt-3	3n	Rb(2.3) × 2, T(15;8), T(18;3), T(X;18)	nd	nd	nd

[a]Brt-1 and brt-5 were analysed at passage 0 and passage 31. [b]Ploidy was determined using the median copy # for each chromosome. [c]Recurrent aberrations were defined as present in 2 or more metaphases, nd, not determined. [d]A probe for the entire sequence of chr 11 was used to confirm aberrations and copy #. '?' indicates that the partner chromosome was not identified in this experiment. [e]A probe for the *Trp53* gene was cohybridized with the chromosome 11 paint probe. [f]A probe for the *Erbb2* gene was cohybridized with the chromosome 11 paint probe

of chromosome instability, the population of cells was mainly clonal and the CGH profile is in good agreement with the aberrations detected by SKY. For example, chromosome 9 material containing the centromere is found in a dicentric chromosome in which a portion of chromosome 8 is inserted, in a translocation with chromosome 6, and in a chromosome 9, which has an insertion of chromosome 6 material (Figure 2). Accordingly, the CGH profile for this tumor (brt-2) shows a gain of the proximal region of chromosome 9 (Figure 1). Similarly, SKY indicates that there is an extra copy of chromosome 15 relative to the ploidy of the cell (Figure 2), and the CGH profile shows a gain of chromosome 15 (Figure 1). The representative metaphase in Figure 2 does not contain the extra copies of chromosome 11 material seen in other cells of this tumor. However, FISH with chromosome painting probes indicated additional small fragments containing chromosome 11 (Table 1). Moreover, the metaphase does show evidence for chromosome 11 instability: one copy of the chromosome is in the process of re-arranging with chromosome 13 (Figure 2a, b).

In tumor brt-1, we could compare SKY data from both early and late passages. Although the majority of cells increased in ploidy from 2n to ranging from 3n–4n after 31 passages, the T(7;11) was retained (Table 1). A whole chromosome paint for chromosome 11 revealed additional copies of a Del(11), which preserved the distal portion of that chromosome including the *Erbb2* locus (see FISH results below). Therefore even a primary tumor without a chromosome 11 gain (Figure 1) eventually selected for the amplification of distal chromosome 11 when passaged in culture.

Two tumors, pbrt-1 and pbrt-3, that arose in *Brca1$^{Ko/Co}$Wap-CreTrp53$^{+/-}$* mice were analysed by SKY (Table 1). Although these tumors both contained

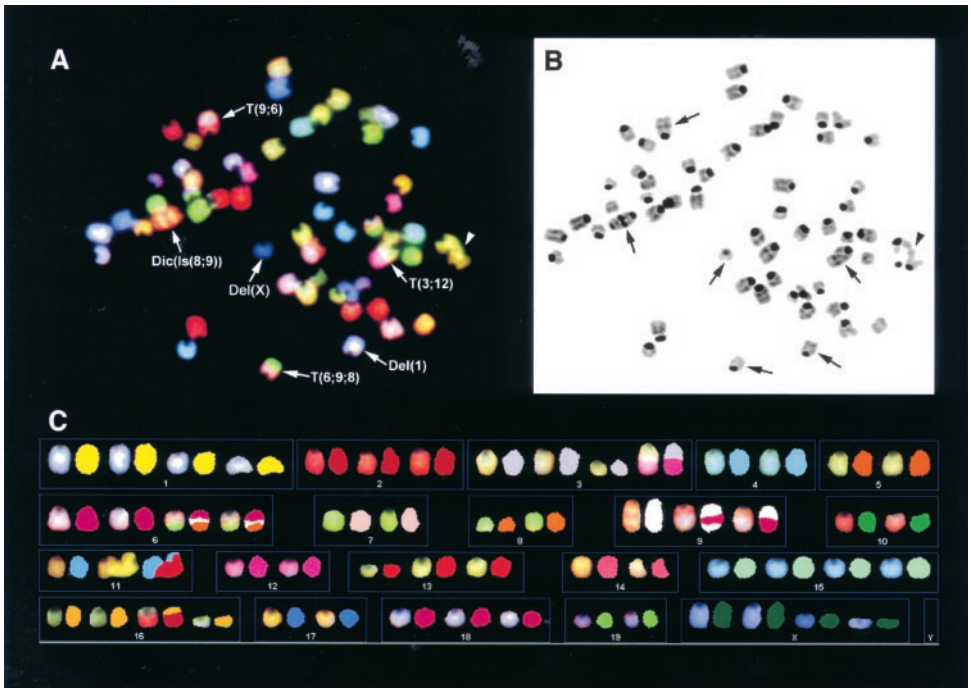

Figure 2 SKY analysis of a representative metaphase from tumor brt-2. The display (RGB) colors are shown in (**a**), the corresponding inverted DAPI image in (**b**), and the full karyotype with display colors on the left of the spectrally-classified chromosomes in (**c**). White arrows indicate the aberrant chromosome 9 structures, and the arrowhead indicates chromosomes 11 and 13 in the process of rearranging, as described in the text. The complete karyotype of this tumor is 56,XXXX, Del(1)x2, Del(2)x2, Del(3), T(3;12), T(6;9;8)x2, Is(6;9), Dic(Is(8;9)), T(9;6), Del(13), Dic(16;2), T(16;19), Del(X)x2, +1, +6, +15, +16, −4, −5, −7, −8, −10, −11, −12, −14, −17, −19

chromosomal aberrations that were present in more than one cell, the degree of chromosomal instability in both made it difficult to reconcile all structural aberrations with the gains and losses seen by CGH (Figure 1). Pbrt-1 had an average of six unique structural aberrations per metaphase cell, and pbrt-3 had an average of four unique aberrations. This is different from tumor brt-2, described above, which had multiple aberrations that were present in every cell. Despite this degree of instability, pbrt-1 displayed a gain of distal chromosome 11, as found in the majority of the *Brca1*-deficient tumors by CGH and SKY (Table 1). A small deleted chromosome 11 is present in several copies in most of the cells (Table 1). As it is found in both triploid and tetraploid cells from pbrt-1, it is likely that the acquisition of the Del(11) preceded the tetrapolidization of the genome and was therefore an early event in tumorigenesis. The detailed karyotype description of the cell lines can be retrieved from the database at: www.ncbi.nlm.nih.gov/sky/skyweb.cgi

FISH analysis indicates that gain of distal chromosome 11 occurs by several mechanisms

CGH and SKY analysis of the *Brca1* conditional mammary tumors indicated that chromosome 11 was frequently involved in structural aberrations which resulted in copy number decreases for proximal 11 and increases for the distal portion of this chromosome. To further elucidate the region of gain, loss, or rearrangement, we combined whole chromosome painting with gene-specific FISH probes for *p53* and/or *Erbb2*. Gain of *Erbb2* (and potentially other breast cancer-specific oncogenes on distal mouse chromosome 11) and the simultaneous deletion of p53 are accomplished via complex chromosomal rearrangements. The results (shown in Figure 3 and described in Table 1), corresponded well with the CGH data. In each case we confirmed the gain of the distal chromosome 11. For example, tumor brt-9 appeared to have a copy number gain of chromosome 11 that included the *Erbb2* gene, which maps to 11D (Figures 1 and 3). SKY and whole chromosome painting combined with the *Erbb2* probe showed that brt-9 has two clones, both of which exhibit two copies of a Del(11) in addition to at least one normal copy (Table 1). Clone *b* contains in addition two translocations involving the proximal and distal portions of chromosome 11, respectively (Table 1). *Erbb2* is present on each Del(11) in both clones, indicating that this aberrant chromosome is derived from an interstitial deletion of bands B–C. *Erbb2* is also present on the distal translocated portion of chromosome 11 in clone *b* (Figure 3) indicating that the breakpoint is proximal to *Erbb2* in this case. Similarly, the gain of 11D-E observed by CGH in tumor brt-5 is due to 1–3 extra copies of an aberrant chromosome 11 with an interstitial deletion of bands B–C (Table 1).

Conversely, tumour brt-2 showed a gain of chromosome 11 by CGH that appeared to be distal to the

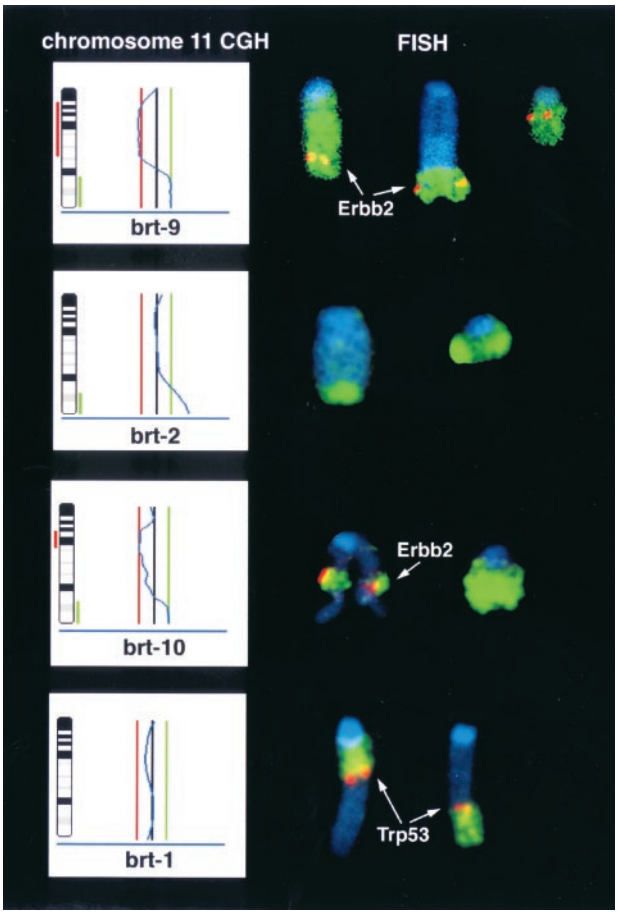

Figure 3 Chromosome 11 aberrations detected by CGH, chromosome painting and FISH probes for *Erbb2* and *p53*. The chromosome 11 panels on the left side of the figure are taken from the original CGH profiles of the tumors indicated. The center line (black) indicates a ratio of 1, and the two adjacent lines denote the threshold values for loss (left, in red) or gain (right, in green) of genetic material. The right panel displays representative FISH analyses of chromosome 11 from the same tumors using a whole chromosome 11 painting probe (green) and BAC clones for *Erbb2* and *p53* (red). Note that the copy number increase in brt-9 includes *Erbb2*, but not in tumor brt-2 and brt-10. The distinctly different probe signals for *p53* in brt-1 indicate the disruption of this gene by chromosomal translocation

Erbb2 gene locus, encompassing band 11E only (Figures 1 and 3). FISH analysis revealed that indeed there are extra copies of a small deleted chromosome 11 relative to the ploidy (triploid) of the tumor (Table 1). We could show that this Del(11) did not contain the *Erbb2* locus by FISH analysis (Figure 3). By CGH, the profile for chromosome 11 in brt-10 appeared similar to that of brt-2 in that the gain of the distal region was limited to 11E (Figures 1 and 3). However, in this case the FISH analysis revealed (in both of the two clones identified) that *Erbb2* is not gained relative to the copy number of chromosome 11, because it is located on the portion of chromosome 11 that is deleted by way of a structural aberration. For example, in clone *b*, which is triploid, there is one copy of a 'normal' chromosome 11, 2 Del(11), two translocations involving the distal region of 11, and one insertion of a portion of chromosome 11 into another chromosome (Table 1). *Erbb2* is present on the translocated pieces of chromosome 11 and on the small insertion, but not on the Del(11), and not on the chromosome 11 that appears to be of normal size by painting, but which must have a small deletion in the *Erbb2* band region (Figure 3). Therefore, the mechanism for the gain of distal chromosome 11 does not always involve gain of *Erbb2*, but always include the region directly distal to that gene.

To confirm that the structural aberrations were distal to the location of the tumor suppressor gene *p53* (11B2-C) we analysed four tumors with a FISH probe for *p53*. Three of these tumors (brt-2, -5 and -10) showed gain of chromosome 11 by CGH, and one did not (brt-1). The results indicate that *p53* was excluded from the copy number increases of distal chromosome 11 as it was observed only on the normal copy of the chromosome in these tumors and not on any of the deleted or translocated portions (Table 1). *p53* was also present on the normal-size chromosome in brt-10 that was deleted for *Erbb2*. Tumor brt-1 showed no copy number change of chromosome 11 by CGH, but SKY analysis revealed a reciprocal T(7;11) in every cell (Table 1). By FISH analysis, we confirmed that *p53* is likely to be at the breakpoint of the clonal translocation observed by SKY (Figure 3) because the probe signals are on either side of the translocated chromosome 11 and also differ in size. This evidence supports our previous results, which had indicated that the p53 transcript size was abnormal in tumor brt-1 (Xu *et al*., 1999a). Although p53 inactivation seems to occur via chromosome translocation in this tumor, additional mechanisms other than chromosomal translocations may be responsible for p53 mutation in *Brca1*-deficient mammary tumors (Xu *et al*., 1999a; and see below).

Western blot analysis reveals aberrant p53 expression in some tumors

To determine whether the expression of p53 was changed even in cases where the gene did not appear to be deleted or rearranged by FISH analysis, we prepared protein extractions from several tumors, both $Brca1^{Ko/Co}$*Wap-Cre* and $Brca1^{Ko/Co}$*Wap-CreTrp53*$^{+/-}$ from which it had been possible to maintain the cells in culture for 20–30 passages (Figure 4). Brt-1 produced no detectable protein product. Similarly, no p53 product was observed from the brt-9 or pbrt-3 cells. Although the α-tubulin control indicates that less protein may have been loaded in lanes 1, 3 and 4, we have performed the experiment several times, also using an antibody for actin detection as yet another control, and have never detected protein in brt-1, pbrt-3 or brt-9 (data not shown). As described previously, brt-1 displayed a rearranged *p53* gene by FISH analysis (Table 1) and by Northern blot analysis of its transcript (Xu *et al*, 1999a). Although it appears that no protein product is produced, we cannot rule out the possibility of a mutant (fusion) protein, which the p53

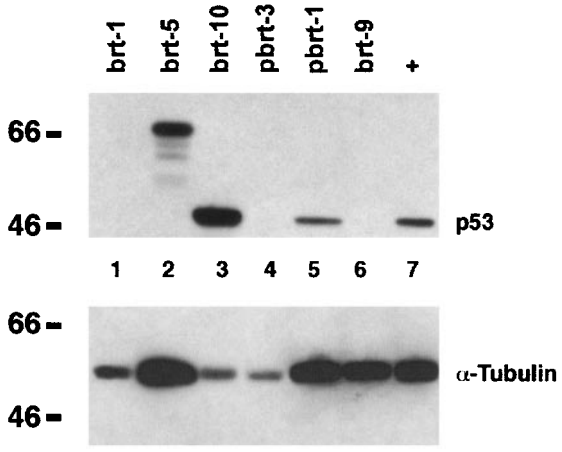

Figure 4 Western immunoblot analysis to detect p53 in *Brca1*$^{Ko/Co}$ tumor cell lines. Total protein for each cell line in lanes 1–6 was detected with antibody to p53. Lane 7 contains protein from MEFs that are known to express p53 as a positive control (see Materials and methods). The membrane was stripped and probed with an α-tubulin antibody to control for protein loading

antibody does not recognize. Chromosome rearrangements are also a likely cause of p53 loss in brt-9: this tumor displayed a gain of chromosome 11 distal to *p53* by CGH, and SKY revealed the gain was due to translocations and interstitial deletions of chromosome 11. Brt-5 appeared to express a mutant version of p53 greater than 64 kD. This tumor exhibited a deleted chromosome 11, which results in the loss of the *p53* gene (Table 1). The mutant p53 protein must be the result of a gene rearrangement that was too small to visualize by cytogenetic techniques. Interestingly, two cell lines (brt-10 and pbrt-1) representing the $p53^{+/+}$ and $p53^{+/-}$ genetic backgrounds, respectively, appeared to express p53 protein products of normal size, although p53 is expressed at a higher level in brt-10 relative to pbrt-1 and to the positive control.

Centrosome abnormalities and aberrant mitoses likely contribute to chromosome instability

We have shown previously that MEFs carrying a targeted deletion in the *Brca1* gene contain multiple functional centrosomes, which result in multipolar and catastrophic mitoses (Xu *et al*., 1999b). To examine whether the mammary tumor cells lacking Brca1 exhibit a similar phenotype, we stained tumor cells from four tumors (brt-1, -2, -9, -10) with an antibody against the γ-tubulin component of the centrosome. We found that 25% of tumor cells contained an abnormal number of three or more centrosomes. The simultaneous stain for DNA clearly showed that these supernumerary centrosomes caused unequal segregation of chromosomes and multipolar mitoses (Figure 5a,b). In addition to its ability to nucleate microtubules, another criterion for an intact centrosome is that it should contain two centrioles. To examine the supernumerary centrosomes in greater detail, we performed electron microscopy on cells from tumor

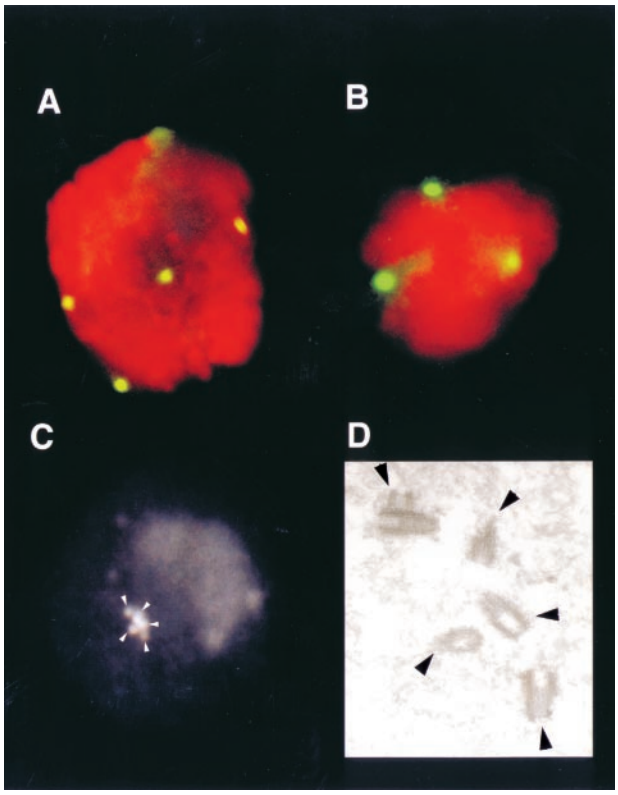

Figure 5 Centrosome amplification in *Brca1*$^{Ko/Co}$ mammary tumors. (**a**, **b**) Tumor cells growing in culture were stained with an antibody against γ-tubulin (green). The DNA counterstain is displayed in red. Cells from tumor brt-1 (**a**), brt-2 (**b**), and brt-10 (**c**; shown in grayscale) display 5, 3, and 5 centrosomes, respectively. (**d**) The same cell shown in (**c**) was analysed by electron microscopy after relocation of γ-tubulin signals. Arrows in (**c**) indicate the individual centrosomes and the corresponding centriole pair(s) in (**d**). The pair on the top left is the most clearly visible; note that this is a cross-section through the cell and the visualization of all pairs would require a series of images

brt-10 in which the centrosomes had been detected earlier using a glutaraldehyde-stable antibody against γ-tubulin. After relocation of the fluorescent signals and acquisition of images from multiple image planes, we could show that each centrosome detected by the anti-γ-tubulin antibody contained normal centrioles (Figure 5c,d). The centrioles in the cells with additional centrosomes did not appear different than those in the cells with only two centrosomes (data not shown).

Discussion

The conditionally mutant *Brca1* mouse was created as a model for inherited human breast cancer (Xu *et al*., 1999a). Previous studies have shown that these mice develop mammary tumors after a long latency, which is decreased in a p53 mutant background. We have now performed molecular cytogenetic analysis on a series of mammary tumors from these mice in order to assess whether the strictly conserved distribution of genomic imbalances observed in human breast cancers is

maintained in this mouse model. This would support its use as a tool to study breast tumorigenesis. We found that all tumors exhibit chromosome instability as evidenced by structural chromosomal aberrations and aneuploidy, yet that they display a pattern of chromosomal gain and loss that is similar to the pattern observed in human breast carcinomas, and in particular to *BRCA1*-associated tumors. Although *Brca1* mutant embryonic cells exhibit random chromosome aberrations and early lethality, deficiency of *Brca1* in the mammary gland allows for the selection of specific genetic changes and subsequent malignant transformation.

Comparative maps of the human and murine genome allowed us to compare the distribution of genomic imbalances between human and mouse. For example, the commonly gained region on chromosome 11 centered on bands 11D-E, a region that is orthologous to human chromosome 17q11-qter, which is frequently amplified in human breast carcinomas (Bieche and Lidereau, 1995; Ried *et al*., 1995; Barlund *et al*., 1997). Of note, the amplicon on chromosome band 17q23, associated with poor prognosis in human cancers, was recently shown to have a limited number of highly expressed genes that may contribute to the more aggressive phenotype (Monni *et al*., 2001). Another analogy extends to the c-*Myc* oncogene, another common target for amplification in human breast cancer, both in sporadic and *BRCA1*-mutation associated tumors (Nass and Dickson, 1997). As shown in our analysis, the locus containing the c-*Myc* gene in the mouse (15D2-D3) is subject to recurring copy number increase in the *Brca1*-deficient mouse tumors. Interestingly, analysis of mouse mammary tumors resulting from overexpression of a c-*Myc* transgene also revealed a copy number gain of the distal region of chromosome 11 (Weaver *et al*., 1999).

Although the chromosome regions appearing as gains by CGH are large, recent studies in which genomic gains and losses have been compared to tumor gene expression profiles have shown that in fact very few genes are both amplified and overexpressed in these regions (Phillips *et al*., 2001; Platzer *et al*., 2002). The comparative mapping of genomic imbalances in human and murine tumors supports this view: despite a frequent gain of the entire long arm of chromosome 8 in human breast carcinomas, not all chromosomal segments of the mouse genome that are orthologous to human chromosome 8 are present in increased copy numbers. In fact, only the segments on murine chromosome 15 are amplified. This finding suggests that indeed oncogenes that reside on human chromosome 8 segments that are present on mouse chromosome 15 are required for tumorigenesis. The c-*Myc* oncogene is obviously a likely candidate.

Our results from the mouse *Brca1* model can also be specifically compared to the distribution of chromosome gain and loss in human breast cancers from *BRCA1* carriers. Tirkkonen *et al*. (1997) found recurring copy number increases on chromosome band 17q22-24 and chromosome arms 8q and 1q. The 8q gain is likely due to c-*Myc* amplification as seen in the *Brca1*-deficient mice, and it is reasonable to suspect that the crucial gene(s) amplified on 17q are homologues of those on mouse 11D-E. Similarly, chromosome 13q exhibited loss in a majority of the *BRCA1* cancers, and the region of mouse chromosome 14 commonly lost in the *Brca1*-deficient tumors is homologous to 13q. The most frequent loss found in the human *BRCA1* breast cancers was mapped to chromosome 5q. Several mouse chromosomes have homology to 5q so a direct comparison is difficult; however it is interesting that the common region of mouse chromosome 11 loss in five tumors (band 11A5) is orthologous to human 5q35 and one can speculate that this chromosome band is the target for loss in human cancers. Progress in the mouse genome sequencing efforts and the development of precise maps of homology will continue to facilitate efforts for comparative molecular cytogenetic studies.

The genomic instability present in these tumors was best visualized by SKY. By analysing multiple metaphases for each tumor it became clear that new structural aberrations are continuously arising as the cells are dividing. Every tumor displayed structural aberrations, numerical chromosomal abberations and multiple clones. Even though the ploidy varied within some tumors, the recurrent marker chromosomes were replicated along with the chromosomal complement, and therefore resulted in overall copy number changes. Analysis of the specific chromosome regions involved in the most recurrent rearrangements enables us to elucidate the mechanism behind the gains and losses found in the CGH profiles.

In the case of the distal region of chromosome 11, SKY revealed a Del(11) in several tumors, and we used gene-specific probes to show that an interstitial deletion occurred in that chromosome. Whole chromosome painting indicated that the region of chromosome 11 that shows a copy number increase by CGH is gained relative to the ploidy of individual tumor cells, and gene-specific FISH showed that the region does not always include the *Erbb2* gene, but always includes the band distal to that gene. Although the *Erbb2* gene is amplified in many somatic breast carcinomas, evidence suggests that this locus is not commonly gained or overexpressed in *BRCA1*-related breast or ovarian cancers (Tirkkonen *et al*., 1997; Rhei *et al*., 1998; Vaziri *et al*., 2001). Studies that correlate gene amplification with gene overexpression point to another gene on 17q23, orthologous to mouse 11D-E (Wu *et al*., 2000; Monni *et al*., 2001). Therefore this model could be used to confirm the relevance of candidate genes in human *BRCA1*-related breast cancer.

Taken together, the CGH and SKY data show that the average number of chromosomal aberrations in these tumors is similar to the number observed in human cancers. Aneuploid breast carcinomas show an ANCA of 6.8-12 (Ried *et al*., 1999). By CGH we observed an ANCA of 8.1 for the *Brca1*-deficient mammary tumors. This number is higher than in

murine tumors induced by overexpression of an oncogene, such as in MMTV-c-*myc* (ANCA = 5.5) or *Erbb2* (ANCA-2.7) transgenics (Weaver *et al*., 1999; Montagna *et al*., 2002). Conditional knockout of the *Brca1* tumor suppressor gene may more closely model familial breast cancer as the second allele is only mutated as the mice reach maturity (Xu *et al*., 1999a). During the long latency, additional genetic changes occur which eventually leads to tumor formation. In the transgenic mice, tumor induction via a strong oncogenic stimulus may circumvent the need for the acquisition of tumor-specific patterns of chromosomal aneuploidies. With the recent success of the Cre-loxP technology, it may become easier to create conditional tumor suppressor gene deletion models that more closely reflect the nature of multi-step carcinogenesis that we observe in human epithelial cancers.

The development of mammary tumors conditionally deleted for *Brca1* is accelerated in a $p53^{+/-}$ background (Xu *et al*., 1999a). It has also been found that haploid loss of p53 can completely rescue the embryonic lethality caused by the $Brac1^{\Delta 11/\Delta 11}$ mutation by way of reduced apoptotic response and impaired G1-S checkpoint control (Xu *et al*., 2001). Clearly, interactions between p53 and Brca1 are important for the maintenance of genomic stability. *BRCA1*-related familial breast cancers are known to contain a higher frequency of *TP53* alterations than sporadic breast and ovarian tumors. Null mutations, as well as mutations that result in the accumulation of p53, have been found. However, although *TP53* mutations clearly occur more often in *BRCA1*-associated tumors than in sporadic breast cancers, no absolute requirement for *TP53* mutation has been proven (Schuyer *et al*., 1999). Three of the murine tumors analysed in this study produced no detectable p53 protein, which was in at least one case (brt-1) due to rearrangement of the gene. Still, we did detect p53 protein of the expected size in two tumors, brt-10 and pbrt-3 (which were germline wild-type and heterozygous mutant for *p53*, respectively). We cannot rule out that these proteins contain deregulating point mutations, as the p53 protein was found to have decreased stability even in $Brca1^{ko/ko}$ $p53^{+/+}$ thymocytes (Xu *et al*, 1999a). During the long latency to tumor formation the severe genomic instability in these tumors may also cause the disruption of other genes in the p53 pathway, for instance *p21*. However, these tumors might provide evidence that tumorigenesis can occur even in the presence of wild-type p53.

We have previously shown that fibroblasts from *Brca1* null embryos exhibit abnormal numbers of centrosomes, aneuploidy, and are deficient in the G2-M checkpoint. Dual immunostaining for γ- and α-tubulin also revealed that the amplified centrosomes could nucleate tubulin and organize spindle poles (Xu *et al*., 1999b). Now we find that *Brca1*-deficient mammary tumor cells maintain this centrosome amplification. By electron microscopy, the centrioles appear structurally normal, unlike those in aneuploid colorectal cancer cell lines, where the absence of colocalization of γ-tubulin positive spots with centrioles correlate with the presence of non-functional centrosomes and the absence of multipolar mitoses (M Difilippantonio *et al*, submitted). We have shown earlier that amplified centrosomes are already present in the earliest $Brca1^{-/-}$ embryonic cell divisions (Xu *et al*., 1999b). This suggests that the segregation defects associated with supernumerary functional centrosomes in this mouse model of breast cancer may indeed contribute to the generation of aneuploidy. BRCA1 colocalizes with the centrosome during mitosis and coimmunoprecipitates with γ-tubulin, a centrosomal component essential for nucleation of microtubules (Hsu and White, 1998). The absence of BRCA1 could therefore directly trigger the emergence of centrosome abnormalities.

We conclude that this comprehensive characterization of chromosomal and genetic defects in mammary gland adenocarcinomas in mice conditionally deficient for *Brca1* has established firm evidence of the similarity with human breast cancers. This extends from the identification of a pattern of genomic imbalances conserved across species from mice to men, to the confirmation of loss of p53 in *BRCA1*-associated tumorigenesis, and to the description of multiple functional centrosomes that induce aneuploidy. Such analyses validate murine experimental tumor sysems as germane models for human cancer.

Materials and methods

Cell culture

For short-term culture, the tumors were minced with scalpel blades, digested in 0.5 mg/ml collagenase type III (Invitrogen, Carlsbad, CA, USA) in modified IMEM medium (Invitrogen) for 5 h to overnight. The cells were then washed twice and resuspended in modified IMEM + 2.5% FBS. Seven of the tumors were harvested for metaphase chromosome preparation (see below) at 48–72 h. For long-term culture, cells were maintained in modified IMEM + 2.5% FBS and cleared of contaminating fibroblasts by differential trypsinization.

SKY and FISH

Metaphase chromosomes for SKY were prepared from tumor cells at passage 0–2. Cells in culture were incubated for 5 h in 0.02 μg/ml Colcemid (Invitrogen), 30 μg/ml bromodeoxyuridine (Sigma, St. Louis, MO, USA) and 0.15 μg/ml fluorodeoxyuridine (Sigma). The cells were lysed in hypotonic solution (0.06 M KCl) and the chromsomes were fixed in methanol:acetic acid (3:1). Spectral karyotyping was performed as described previously (Liyanage *et al*., 1996; Weaver *et al*., 1999). For each tumor, at least five metaphases were analysed.

Mouse *p53* and *Erbb2* BAC clones were obtained from a Genome Systems (St Louis, MO, USA) library screen using gene-specific primers. Both the *Erbb2* and the *p53* BACs were labeled by nick-translation with Spectrum Orange dUTP (Vysis, Downers Grove, IL, USA). Chromosome 11 was similarly labeled directly with dUTP-Cy5 or indirectly with biotin-16-dUTP (Roche Biomolecular, Indianapolis, IN, USA) and detected with FITC conjugated to avidin (Vector Laboratories, Burlingame, CA, USA). The SKY and CGH

results can also be viewed at www.ncbi.nlm.nih.gov/sky/skyweb.cgi.

CGH

Genomic DNA from primary tumors was extracted following standard procedures. DNA labeling, hybridization and detection were performed as described (Weaver *et al*., 1999). Images were acquired with a Leica DMRXA epifluorescence microscope (Leica, Wetzlar, Germany) using fluorochrome-specific filters (Chroma Technologies, Brattleboro, VT, USA) and analysed with Leica QCGH software.

Immunocytochemistry

Cells seeded overnight in Falcon chamber slides (Fisher Scientific, Santa Clara, CA, USA) were fixed in 2.5% paraformaldehyde in 5 mM $MgCl_2$/PBS for 15 min at room temperature, washed in 0.3 M glycine in 1 × PBS, permeabilized in 0.2% Triton X-100 in 1 × PBS, and incubated overnight with polyclonal rabbit anti-γ-tubulin T3559 (Sigma) diluted 1:1000 in 5% goat serum in 1 × PBS. The antibody complexes were detected with FITC-conjugated goat anti-rabbit IgG (Roche Biomolecular) and stained with DAPI. Gray-level images were acquired on a Leica DMRXA epifluorescence microscope using Leica QFISH software and pseudocolored (Leica Imaging Systems, Cambridge, UK).

Electron microscopy

Cells were grown on gridded coverslips and fixed in cytoskeleton buffer using standard procedures (Spector *et al*., 1997). Immunodetection was performed as described above, except using glutaraldehyde stable monoclonal mouse anti-γ-tubulin T6557 (Sigma) diluted 1:1000 in 5% goat serum in PBS, followed by incubation with FITC-conjugated sheep anti-mouse IgG (Roche Biomolecular) as the secondary antibody. Cell nuclei were counterstained with DAPI. Cells with aberrant numbers of γ-tubulin staining bodies were imaged and their coordinates recorded. The cells were then relocated and thin sections were examined using a Hitachi H-7000 transmission electron microscope operated at 75 kV.

Western blot analysis

Five to 8×10^6 cells were lysed in 0.5% Triton X-100 buffer (Bacon *et al*., 1995). For Western blot analysis of cell lysates, 100 μg of protein from each sample was subjected to PAGE on a 10% SDS-polyacrylamide gel and transferred to Immobilon (Millipore Corp., Bedford, MA, USA) and immunoblotted using a monoclonal anti-p53 (Zymed, San Francisco, CA, USA) or anti-α-tubulin (Sigma) antibodies. Bands were localized with the enhanced chemiluminescence system (Amersham Pharmacia, Buckinghamshire, UK). As a positive control for the p53 antibody in mouse cells, we used mouse embryonic fibroblasts containing the oncogene E1a, which elevates p53 levels (kindly provided by Kevin Ryan). Details for all protocols can be retrieved from the following website: http://www.riedlab.nci.nih.gov/.

Acknowledgments
The authors wish to thank Buddy Chen for manuscript editing, Joseph Cheng for IT-support and David L Spector for helpful discussions.

References

Bacon CM, Tortolani PJ, Shimosaka A, Rees RC, Longo DL and O'Shea JJ. (1995). *FEBS Lett.,* **370,** 63 – 68.
Barlund M, Tirkkonen M, Forozan F, Tanner MM, Kallioniemi O and Kallioniemi A. (1997). *Genes Chromosomes Cancer,* **20,** 372 – 376.
Bieche I and Lidereau R. (1995). *Genes Chromosomes Cancer,* **14,** 227 – 251.
Bochar DA, Wang L, Beniya H, Kinev A, Xue Y, Lane WS, Wang W, Kashanchi F and Shiekhattar R. (2000). *Cell,* **102,** 257 – 265.
Deng CX and Brodie SG. (2001). *Semin. Cancer Biol.,* **11,** 387 – 394.
Deng CX and Scott F. (2000). *Oncogene,* **19,** 1059 – 1064.
Ghadimi BM, Schrock E, Walker RL, Wangsa D, Jauho A, Meltzer PS and Ried T. (1999). *Am. J. Pathol.,* **154,** 525 – 536.
Gowen LC, Johnson BL, Latour AM, Sulik KK and Kollar BH. (1996). *Nat. Genet.,* **12,** 191 – 194.
Hakem R, de la Pompa JL, Sirard C, Mo R, Woo M, Hakem A, Wakeham A, Potter J, Reitmair A, Billia F, Firpo E, Hui CC, Roberts J, Rossant J and Mak TW. (1996). *Cell,* **85,** 1009 – 1023.
Hsu L-C and White RL. (1998). *Proc. Natl. Acad. Sci. USA,* **95,** 12983 – 12988.
Khanna KK and Jackson SP. (2001). *Nat. Genet.,* **27,** 247 – 254.
Liu CY, Flesken-Nikitin A, Li S, Zeng Y and Lee WH. (1996). *Genes Dev.,* **10,** 1835 – 1843.
Liyanage M, Coleman A, du Manoir S, Veldman T, McCormack S, Dickson RB, Barlow C, Wynshaw-Boris A, Janz S, Wienberg J, Ferguson-Smith MA, Schrock E and Ried T. (1996). *Nat. Genet.,* **14,** 312 – 315.
Ludwig T, Chapman DL, Papaioannou VE and Efstratiadis A. (1997). *Genes Dev.,* **11,** 1226 – 1241.
Monni O, Barlund M, Mousses S, Kononen J, Sauter G, Heiskanen M, Paavola P, Avela K, Chen Y, Bittner ML and Kallioniemi A. (2001). *Proc. Natl. Acad. Sci. USA,* **98,** 5711 – 5716.
Montagna C, Andrechek ER, Padilla-Nash H, Muller WJ and Ried T. (2002). *Oncogene,* **21,** 890 – 898.
Nass SJ and Dickson RB. (1997). *Breast Cancer Res. Treat.,* **44,** 1 – 22.
Phillips JL, Hayward SW, Wang Y, Vasselli J, Pavlovich C, Padilla-Nash H, Pezullo JR, Ghadimi BM, Grossfeld GD, Rivera A, Linehan WM, Cunha GR and Ried T. (2001). *Cancer Res.,* **61,** 8143 – 8149.
Platzer P, Upender MB, Wilson K, Willis J, Lutterbaugh J, Nosrati A, Willson JK, Mack D, Ried T and Markowitz S. (2002). *Cancer Res.,* **62,** 1134 – 1138.
Rhei E, Bogomolniy F, Federici MG, Maresco DL, Offit K, Robson ME, Saigo PE and Boyd J. (1998). *Cancer Res.,* **58,** 3193 – 3196.
Ried T, Heselmeyer-Haddad K, Blegen H, Schrock E and Auer G. (1999). *Genes Chromosomes Cancer,* **25,** 195 – 204.

Ried T, Just KE, Holtgreve-Grez H, du Manoir S, Speicher MR, Schrock E, Latham C, Blegen H, Zetterberg A, Cremer T and Auer G. (1995). *Cancer Res.,* **55,** 5415–5423.

Schuyer M and Berns EM. (1999). *Mol. Cell Endocrinol.,* **155,** 143–152.

Schuyer M, Henzen-Logmans SC, van der Burg ME, Fieret JH, Derksen C, Look MP, Meijer-van Gelder ME, Klijn JG, Foekens JA and Berns EM. (1999). *Eur. J. Obstet. Gynecol. Reprod. Biol.,* **82,** 147–150.

Shen SX, Weaver Z, Xu X, Li C, Weinstein M, Chen L, Guan XY, Ried T and Deng CX. (1998). *Oncogene,* **17,** 3115–3124.

Spector DL, Goldman RD and Leinwand LA. (1997). *Cells: A Laboratory Manual.*. Cold Spring Harbor Laboratory Press.

Tirkkonen M, Johannsson O, Agnarsson BA, Olsson H, Ingvarsson S, Karhu R, Tanner M, Isola J, Barkardottir RB, Borg A and Kallioniemi OP. (1997). *Cancer Res.,* **57,** 1222–1227.

Tomlinson GE, Chen TT, Stastny VA, Virmani AK, Spillman MA, Tonk V, Blum JL, Schneider NR, Wistuba II, Shay JW, Minna JD and Gazdar AF. (1998). *Cancer Res.,* **58,** 3237–3242.

Vaziri SA, Tubbs RR, Darlington G and Casey G. (2001). *Mol. Pathol.,* **54,** 259–263.

Weaver ZA, McCormack SJ, Liyanage M, du Manoir S, Coleman A, Schrock E, Dickson RB and Ried T. (1999). *Genes Chromosomes Cancer,* **25,** 251–260.

Wu GJ, Sinclair CS, Paape J, Ingle JN, Roche PC, James CD and Couch FJ. (2000). *Cancer Res.,* **60,** 5371–5375.

Xu X, Qiao W, Linke SP, Cao L, Li WM, Furth PA, Harris CC and Deng CX. (2001). *Nat. Genet.,* **28,** 266–271.

Xu X, Wagner KU, Larson D, Weaver Z, Li C, Ried T, Hennighausen L, Wynshaw-Boris A and Deng CX. (1999a). *Nat. Genet.,* **22,** 37–43.

Xu X, Weaver Z, Linke SP, Li C, Gotay J, Wang XW, Harris CC, Ried T and Deng CX. (1999b). *Mol. Cell.,* **3,** 389–395.

Zhong Q, Chen CF, Li S, Chen Y, Wang CC, Xiao J, Chen PL, Sharp ZD and Lee WH. (1999). *Science,* **285,** 747–750.